# A Review of the Quantification and Classification of Pigmented Skin Lesions: From Dedicated to Hand-Held Devices

**Mercedes Filho, Zhen Ma and João Manuel R. S. Tavares**[*]

Instituto de Ciência e Inovação em Engenharia Mecânica e Engenharia Industrial,
Departamento de Engenharia Mecânica, Faculdade de Engenharia, Universidade do Porto,
Rua Dr. Roberto Frias, 4200-465, Porto, Portugal
emails: mfilho@inegi.up.pt, zhen-ma@fe.up.pt, tavares@fe.up.pt
[*]corresponding author

**Corresponding author:**

Prof. João Manuel R. S. Tavares

Faculdade de Engenharia da Universidade do Porto (FEUP)

Departamento de Engenharia Mecânica (DEMec)

Rua Dr. Roberto Frias, s/n, 4200-465 PORTO - PORTUGAL

Tel: +315 22 5081487, Fax: +315 22 5081445

Email: tavares@fe.up.pt,

Url: www.fe.up.pt/~tavares

# A Review of the Quantification and Classification of Pigmented Skin Lesions: From Dedicated to Hand-Held Devices

**Mercedes Filho, Zhen Ma and João Manuel R. S. Tavares**[*]

Instituto de Ciência e Inovação em Engenharia Mecânica e Engenharia Industrial,

Departamento de Engenharia Mecânica, Faculdade de Engenharia, Universidade do Porto,

Rua Dr. Roberto Frias, 4200-465, Porto, Portugal

emails: mfilho@inegi.up.pt, zhen.ma@fe.up.pt, tavares@fe.up.pt

[*]corresponding author

**Abstract**

In recent years, the incidence of skin cancer cases has risen, worldwide, mainly due to the prolonged exposure to harmful ultraviolet radiation. Concurrently, the computer-assisted medical diagnosis of skin cancer has undergone major advances, through an improvement in the instrument and detection technology, and the development of algorithms to process the information. Moreover, because there has been an increased need to store medical data, for monitoring, comparative and assisted-learning purposes, algorithms for data processing and storage have also become more efficient in handling the increase of data. In addition, the potential use of common mobile devices to register high-resolution images of skin lesions has also fueled the need to create real-time processing algorithms that may provide a likelihood for the development of malignancy. This last possibility allows even non-specialists to monitor and follow-up suspected skin cancer cases. In this review, we present the major steps in the pre-processing, processing and post-processing of skin lesion images, with a particular emphasis on the quantification and classification of pigmented skin lesions. We further review and outline the future challenges for the creation of minimum-feature, automated and real-time algorithms for the detection of skin cancer from images acquired via common mobile devices.

**Keywords:** Skin lesion; Dermoscopy; Quantification; Classification; Mobile Application

# 1. Introduction

Skin lesions are generally characterized by an abnormal runaway growth of groups of cells on the skin. Depending on their behavior, the lesions may be classified as benign or malignant. Benign lesions show a more ordered and controlled growth, and do not proliferate into other tissues. On the contrary, malignant skin cells (i.e., skin cancer) are generally unlimited in self-growth, and may invade other tissues (i.e., metastasize), even quite distant from the primary initial focus.

Skin cancer is the most common form of cancer, being responsible, globally, for about 40% of all cancer cases [1, 2]. However, it is Australia and New Zealand that show the highest rates of skin cancer [3]. It is known that over 90% of all skin cancer cases are caused by exposure to ultraviolet radiation from the Sun; the increase in skin cancer observed in recent years is mainly related to the thinning and/or depletion of the ozone layer[1,2]. However, artificial ultraviolet exposure (i.e., tanning) is showing an increasing impact on the number of registered skin cancer cases. People with lighter skin and poor imune function are generally more at risk of developing skin cancer[1,2].

The most common forms of skin cancer are (non-melanoma) basal cell cancer and squamous cancer, and melanoma (Fig. 1). The former, non-melanoma forms of skin cancer, are generally highly curable[3]. However, of these three forms, melanoma is the most aggressive; it is most likely to metastasize, and it is associated with the highest mortality (75%) rate[1,2,4] [4]. Despite this, melanoma has one of the highest survival rates among all cancers; about 90% of all UK and USA patients diagnosed with melanoma survive more than 5 years[1,2]. Indeed, the cure rate is highest when caught in the early stages; if the melanoma has metastasized, the prognosis is less favourable.

---

1        http://www.skincancer.org/skin-cancer-information/skin-cancer-facts

2        http://www.cancerresearchuk.org/cancer-info/cancerstats/types/skin

3        http://www.cancer.net/cancer-types/skin-cancer-non-melanoma/statistics

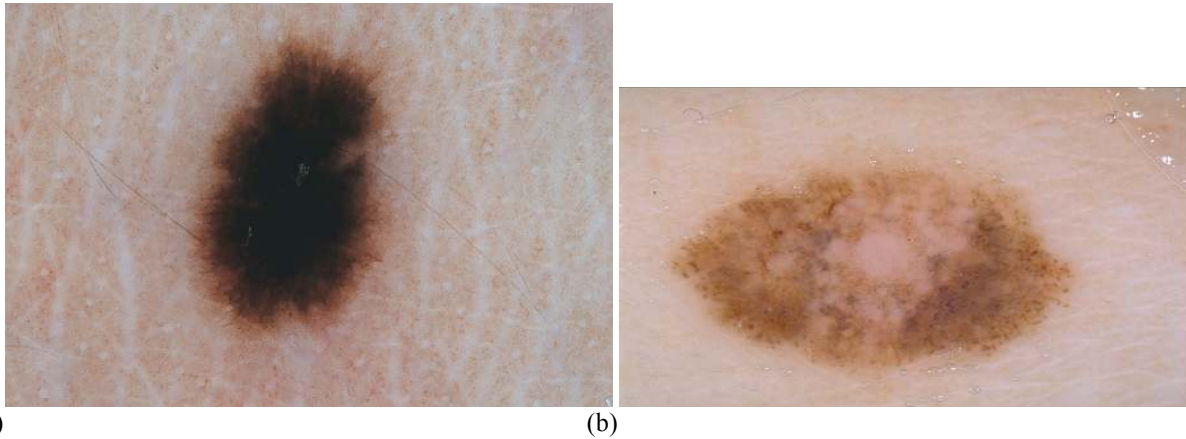4        http://apps.nccd.cdc.gov/uscs

Fig. 1: Skin lesions on dermoscopic images. A (a) benign nevus and a (b) melanoma.

The increased global rate of skin cancer cases calls for the development of computer-assisted algorithms capable of handling large amounts of data, and providing, preferably in real-time and in an automated fashion, a likelihood for the diagnosis of malignancy. This is particularly relevant considering the recent trend for using common mobile devices to acquire images of skin lesions. We here review the major computational methods applied to the pre-processing, processing and post-processing of skin lesion images, stressing the importance of the quantification and classification step in the characterization and diagnosis of pigmented skin lesions.

The paper is organized as follows: in Sections 2, 3 and 4 we review the current state-of-the art in the acquisition, pre-processing and segmentation, respectively, of skin lesion images. In Section 5 we discuss several of the recent applications for skin lesion quantification and classification. Section 6 includes an overview of some of the recent work on hand-held device applications for skin lesion diagnosis. A summary of our findings and future challenges in the field is presented in Section 7.

## 2. Image Acquisition

Confocal scanning laser microscopy (CSLM), optical coherence tomography (OCT), ultrasound, magnetic resonance imaging (MRI), and spectroscopic imaging are examples of non-

invasive techniques that are employed to image skin lesions [5-7]. Clinical (or macroscopic) images and dermoscopy (i.e., dermatoscopy or epiluminescence microscopy) are portable affordable imaging techniques that allow computer-assisted examination and diagnosis of skin lesions[5].

Clinical images are images that are generally acquired via a still camera, such as the common camera or a mobile device (e.g, mobile phones and tablets), or a video camera. However, these images are frequently affected by the presence of artefacts, such as hairs, shadows and lines, by poor resolution, and by variable observing conditions, such as distance and illumination.

Dermoscopy, on the other hand, makes use of a dermatoscope (e.g., Nevoscope[®] from TransLite, LLC, USA), a device that includes a magnifier (e.g., 10x), a non-polarized light source, a transparent plate, and a liquid medium (commonly, immersion oil), that is placed between the instrument and the skin to increase transluscence and decrease skin reflections. Modern dermatoscopes (e.g., Firefly DE350[©] from Firefly Global, USA) employ polarized light instead of a liquid medium to cancel out skin reflections, and highlight the surface pigmentation, sub-surface vasculature and blood flow, while hybrid apparatuses (e.g., DermLite II hybrid M[®] from 3Gen, Inc., USA) combine the clarity of a contact oil immersion device with the practicality of a polarized device.

It has been shown that, with doctors trained in dermoscopic techniques, the diagnostic accuracy, or sensitivity, for melanoma increases by 20%, and specificity increases by 10%, when compared to diagnoses performed with the naked eye [8-10]. On the other hand, modern computer-aided diagnostic tools may now provide sensitivities (86%) and specificities (52%) comparable to sensitivities (85%) and specificities (48%) of the most accurate dermatologists using dermoscopic images [11].

Three-dimensional (3D) dermoscopy is a modern stereovision system that allows volumetric quantification of skin lesions [12]. Recent technology also takes advantage of the portable and

---

5        http://www.anthem.com/medicalpolicies/policies/mp_pw_a049923.htm

affordable aspect of hand-held devices (e.g., mobile phones and tablets), which allow the acquisition of high-resolution images, for skin lesion monitoring and diagnosis. These hand-held devices may be combined with adaptable dermatoscopic equipment for better resolution [13]. In addition, targeted applications for hand-held devices may provide accuracies for malignancy likelihood and processing speeds comparable to common computers [13-18].

## 3. Image Pre-Processing

One of the major challenges in medical data processing is the ability to distinguish between different types of tissues, including diseased tissues, in the human body. This is imperative in order to detect, identify and characterize anomalies in the data that could signal disease, and proceed with a medical diagnosis or prognosis and treatment or excision, if necessary [19].

Identification, or labelling, of different types of human tissue entails, in many instances, a series of pre-processing steps (i.e., image filtering), aimed at enhancing the acquired images, i.e., reduction of the image noise level, smoothing of the image, and increasing the contrast. In the case of skin lesions, linear filters, such as the average filter [20], frequently produce pre-processed images with blurred edges, and the loss of fine detail. The (non-linear) median filter [20], on the other hand, generally adequately removes artefacts (e.g., hair, shadows and lines) while preserving, and sometimes enhancing, region boundaries. Anisotropic diffusion [21], an iterative filtering process, has been shown to be efficient in removing noise, but is less effective than the median filter at enhancing edges. Morphological filtering [22] has been shown to be efficient in reducing the image noise level, and handling of low contrast regions. More recently, bi- and multi-lateral filtering [23-26] have demonstrated an excellent performance in terms of edge preservation, while reducing the noise level in the image (Table 1 and Fig. 2).

| Filtering Method | Reference | Filtering Method | Reference |
|---|---|---|---|
| Average Filter | [20] | Anisotropic Diffusion | [21] |
| Median Filter | [20] | Morphological Filtering | [22] |
| Bi-/Multi-Lateral | [23, 24] | | |

Table 1: Image Pre-Processing – Filters.



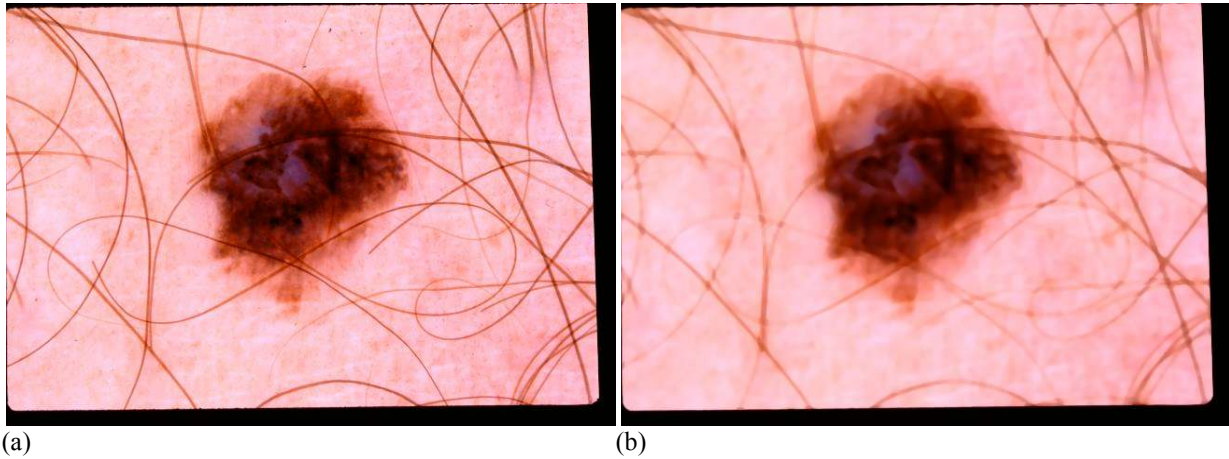(a)                                    (b)

Fig. 2: An illustration of image pre-processing with the median filter to decrease the influence of hair. The (a) original image and the (b) image after smoothing (kernel size = 7).

## 4. Segmentation

After pre-processing, image processing of skin lesions proceeds with the recognition of patterns or regularities in the image and/or the application of rules or checklists to the data, in order to extract, i.e., to segment, the region of interest (ROI), in this case, the skin lesion. This operation generally requires the detection of discontinuities in the data, or the application of similarity criteria to the image, in order to identify the ROI.

Segmentation algorithms [27] may be edge-based [28], i.e., they search for discontinuities in the intensity of the pixels, when compared to pixels in the neighboring regions. However, such algorithms are known to achieve, in many instances, only partial segmentation [22], and must be applied in combination with other segmentation methods to obtain a final adequate result. Canny's edge detector [29] is an example of an edge-based segmentation algorithm [30], which, in combination with iterative filtering [31], has shown promising results for border detection of skin

lesions.

Threshold-based methods [32, 33] use as input the histogram of the image, to which threshold levels (manually or automatically selected) are applied to generate a binary map, where the skin lesion is extracted from the background. An automatic selection of the threshold levels requires supplementary algorithms, such as Otsu's method [34], which employs the normalization histogram to find the optimum threshold level to be applied for lesion segmentation [35].

Region-based segmentation [36] is a technique that establishes regions based on growing or grouping criteria. The data may be initially subdivided into regions, which are then merged together (i.e., grouping), or regions may be grown through the inclusion of additional data into the region (i.e., growing). The Mumford-Shah [37] and Chan-Vese [38] methods are two such examples of region-based segmentation. However, these techniques may have difficulty to handling boundaries of low contrast unless combined with machine-learning techniques [39, 40].

Segmentation may also be achieved through the application of artificial intelligence (AI) principles [41], which are anchored to human-based learning, reasoning and evolution. These methods may be applied by themselves, or in combination with similar AI methods or more traditional segmentation algorithms to provide better segmentation results. As an example, artificial neural networks (ANNs) [42], in combination with Genetic Algorithms (Gas) [43], may provide faster computational speeds and better performances [44].

Segmentation based on active contours [45] is a technique involving the deformation of curves toward the ROI. In parametric deformable models, the curve deformation is driven by energy forces. The internal energy is related to the elasticity and rigidity, and drives the smooth expansion or contraction of the curve. An external energy (manually or automatically selected) counteracts the internal energy, by driving the curve toward the desired borders. The model may also include a global energy, which drives the curve towards relevant features in the image (e.g., lines and

corners). Snake models [45] are traditional parametric deformable models. The gradient vector flow (GVF) [46] is another example of a parametric deformable model, which applies an external energy based on the extrapolation of the gradient vectors to the entire image [47]. However, these models generally do not adequately handle the presence of large curvatures and topological changes. On the other hand, geometric deformable models do track the topological changes of the curve during the segmentation process. The level set [48, 49] and active contours without edges [38] method are two such examples of geometric deformable models. These models are less dependent on the choice of the initial curve, and allow the estimation of the geometrical features of the curve (Table 2).

| Segmentation Method | Reference | Segmentation Method | Reference |
|---|---|---|---|
| *Edge-based* | | *Artificial Intelligence* | |
| Canny's Edge Detector | [29] | Artificial Neural Networks | [42] |
| *Threshold-based* | | Genetic Algorithms | [43] |
| Otsu's Method | [34] | *Active Contours (Parametric)* | |
| *Region-based* | | Snake Models | [45] |
| Mumford-Shah Method | [37] | Gradient Vector Flows | [46] |
| Chan-Vese Method | [38] | *Active Contours (Geometric)* | |
| | | Level Set | [48] |
| | | Active Contours Without Edges | [38] |

Table 2: Image Processing – Segmentation (examples).

Whereas binary logic has been traditionally used in segmentation algorithms, the partial-truth-based fuzzy logic may also be applied to improve segmentation performance. This includes using fuzzy logic with region-based methods [50-53], neural networks [54], and clustering techniques [53], and the use of fuzzy logic to search for the optimal threshold level in threshold-based segmentation [55].

Segmentation algorithms may also be classified as automated (unsupervised learning) or semi-automated (supervised learning). In the latter case, the procedure requires the intervention, at least in an initial phase, of an expert. This may include real-time approximate delineation and/or

identification, with subsequent refinement of the regions through appropriate segmentation algorithms, or the provision of a set of training data, i.e., data which has been à priori correctly labelled by hand, and which is then used as a learning tool to create models of the ROI. An example of a supervised segmentation method is the application of the (non-parametric) K-nearest neighbor (k-NN) algorithm [56] to skin lesion analysis [57], while an example of an unsupervised method [58] is K-means clustering [59] (Fig. 3).



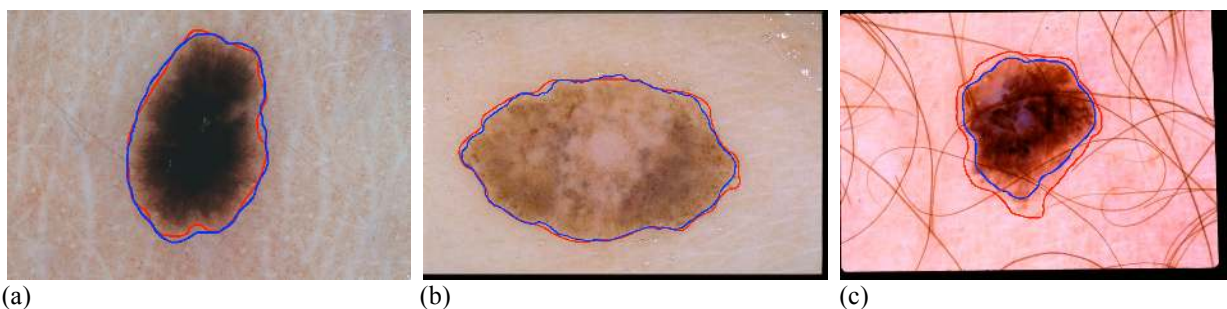(a)                                     (b)                                     (c)

Fig. 3: Segmentation of the images in Figs. 1 and 2 using the algorithm proposed in [60]. The red contours are for the manual segmentation, while the blue contours are results of the algorithm (both contours have a two-pixel width for illustration).

## 5. Quantification and Classification

Once the data is labelled, the ROI may be characterized using parameters such as size, color, texture and shape (i.e., quantification). These parameters are described by a feature vector [61], which contains information that may be classified as categorical or nominal, ordinal, integer-valued or real-valued.

For medical data purposes, one of the simplest quantifications of tissue features is a two-dimensional (2D) description of the shape, texture and color. This is generally employed when a 2D feature description suffices for a medical diagnosis, in the case of flat skin lesions, or when higher computational effort does not justify the increase in sensitivity and specificity.

In order to use color features for the characterization of skin lesions, it is necessary that the characterization be repeatable, i.e., invariant under varying viewing conditions such as surface orientation, illumination direction and illumination intensity, and possess a discriminative power.

Because colors are generally device-dependent, invariant color descriptors can be built on, for example, the CIE-RGB color model and the (perceptually uniform) L*a*b color space (where L is for the perceived lightness, and a and b are for the color-opponent dimensions) [62]. Properties such as saturation, hue, chroma and intensity may be gauged from the color (invariant) spatial derivatives [63]. In addition, color tensor-based features, such as energy, orientation and curvature, may also be derived [63] (Table 3).

| *Color* | | |
| --- | --- | --- |
| Spatial Derivatives | | |
| | | Saturation |
| | | Hue |
| | | Chroma |
| Tensor-Based | | |
| | | Energy |
| | | Orientation |
| | | Curvature |

Table 3: Image Processing - Quantification of color Features (examples).

The ROI shape may be analyzed according to quantitative characteristics, such as compactness and spatial moments, which make use of the geometric and statistical properties of all the pixels within the segmented region. Radial distance measurements, chain codes, differential chain codes and Fourier descriptors, on the other hand, provide shape information based on the parameters of the boundary pixels and closed contours. Branching or elongated structures are best described through the thinning technique, which allows the added computation of lengths, angles, curvature and orientation of the segmented regions.

Compactness [64], defined as $C=P^2/A$ or alternatively, $C'=1-4P/C$ (normalized compactness), employs simple measurements of the perimeter (P) and area (A) of the ROI, to assess how close the shape of the region is to circular; i.e., C increases with shape complexity.

Spatial moments [65] are used to define the shape (on binary and grey-scale images) and

intensity distribution (on grey-scale images) of the segmented region. In particular, it provides information about the orientation or principle axis of the ROI, and its eccentricity. Central moments may be further combined to obtain invariant (i.e., translation, rotation, scale) descriptors. Spatial moments are generally sensitive to ROI size or small substructure; they do not work well when the lesion is less than several pixels wide. However, spatial moments normalized to the standard deviation have been reported to improve classification and sensitivity to noise [66].

Radial distance measurements [67] rely on the characterization of the ROI boundary behavior, after a transformation of the boundary into a one-dimensional (1D) signal. The boundary and variation of the regions, and its curvature, may be analyzed via the centroid and the (normalized) distance to the centroid, and other shape metrics, such as the estimation of entropy and various statistical moments. For example, boundary roughness may be quantified by the number of times the radius crosses its mean, and other metrics. The normalized radial distance sequence may also be analyzed with the wavelet formalism [68, 69], and in the Fourier transform [70] domain; higher value Fourier coefficients provide the shape information.

Chain codes [71], applied on spatially degraded images, provide information on the shape, via the relative position of consecutive points (i.e., 4 or 8 point connectivity) on the boundary. Because chain codes are dependent on the starting point, as a convention, the chain code with the smallest numerical value is chosen. Similarly, differential chain codes probe local boundary smoothness, symmetry and curvature, via the analysis of the difference and comparison between consecutive points of the original chain code. Shape information, which is contained in the low-order coefficients, may be recovered from the Fourier transform [70] of the contour function (the complex sequence of pixels); i.e., coefficient = 0 provides the centroid of the contour and coefficient = 1 provides the radius.

Thinning [72, 73] is a technique that involves creating a skeletal structure from medial lines

via, for example, the estimation of the (minimal) Euclidean distance between interior and boundary pixels. Distances between consecutive pixels on the medial lines may also be used to estimate lengths, and other parameters, such as the curvature and orientation. Because the procedure is computationally heavy (it requires the calculation of many individual distances), algorithms such as the Zhang & Suen algorithm [74] have been developed to minimize the necessary computations (Table 4).

| *Shape* | |
| --- | --- |
| Region-Based | |
| | Compactness |
| | Spatial Moments (Orientation, Eccentricity) |
| Edge-Based | |
| | Radial Distance (Curvature, Entropy, Statistical Moments) |
| | Chain Codes |
| | Differential Chain Codes |
| | Fourier Descriptors |
| | Thinning (Length, Curvature, Orientation) |

Table 4: Image Processing - Quantification of Shape Features (examples).

Texture may be quantified through the analysis of the statistical moments, co-occurrence matrix measures, spectral measures, fractals and run-length statistics. Rough regions will show a wide variety of pixel values, whereas smooth regions will generally show closely placed values.

From the intensity histogram of the data, the second statistical moment about the mean (variance) provides a channel to analyze the visual perception of roughness [75]. The third moment (skewness) is related to asymmetry, whereas the fourth moment (kurtosis) correlates with uniformity [75]. However, because roughness is associated with grain size, statistical moments do not retain spatial information.

Co-occurrence matrix measures [76, 77], obtained from the 2D histogram of the segmented region, provide information on the relative distance and angle between pairs of pixels; i.e., the

second moment (energy) is related to the homogeneity, the third moment (inertia) is related to the texture contrast, the fourth moment (inverse difference) penalizes regions of higher contrast, and the fifth moment (entropy) is related to the level of randomness. Means and standard deviations of marginal distributions derived from the co-occurrence matrix may be used to construct other texture metrics.

When the texture possesses a periodicity or some quasi-periodicity, spectral measures (i.e., spatial frequency and angle) in the Fourier domain [70] provide information on the texture angle, grain size and contrast. The mean, maximum and variance of the spectral measures may provide additional texture descriptors.

Fractals [78] may be used to describe roughness, via the quantification of the fractal dimension; a fractal dimension of two corresponds to a smooth surface, whereas dimensions of higher orders correlate with the degree of roughness. Generally, the fractal dimension is obtained using linear regression analysis (via box counting [79]), maximum likelihood [80] or fractal interpolation functions [81]. Run-length statistics [82] provide information, via consecutive (linear strand) pixels that have the same value. For every angle, the number of runs of a certain length at a certain grey-scale is used to construct a run-length histogram; in a smooth region, there will be more runs at large lengths than in a rough structure. The run percentage, and its mean and standard deviation, may also be used for texture quantification (Table 5).

2D to 3D generalization of feature quantification works by either creating multiple image slices at various depths (that are then treated as volumetric data), or the images may be acquired directly in 3D space (e.g., stereovision dermoscopy, [12]). When a 3D analysis of the features is required, for example, in the case of raised skin lesions, other extraction techniques are employed [12, 83, 84]. One such example is the use of tessellation, which fits the surface of a 3D object with basic 2D shapes (polygons) of equal area, to estimate degrees of anisotropy from the orientation

indicatrice. Fourier descriptors expanded to 3D have also been developed [85], as well as thinning algorithms (Vornoi skeleton concept [86], hybrid thinning [87] and voxel coding [88]).

Once (color, shape, size, texture) features have been determined, for optimization purposes, the features may suffer an extraction (i.e., data compression) or the features may suffer a selection, whereby redundant or irrelevant features are removed (i.e., creation of a data subset or feature selection). Rules, checklists, and sets or groups of different features are created, that optimally combined, provide a diagnosis for malignancy.

| *Texture* | | |
|---|---|---|
| Statistical Moments | | |
| | | Variance |
| | | Skewness |
| | | Kurtosis |
| Co-Occurrence Matrix Measures | | |
| | | Energy |
| | | Inertia |
| | | Entropy |
| Spectral Measures | | |
| | | Angle |
| | | Size |
| | | Contrast |
| Fractals | | |
| | | Dimension |
| Run-Length Statistics | | |
| | | Run Percentage |
| | | Mean |
| | | Standard Deviation |

Table 5: Image Processing - Quantification of Texture Features (examples).

In addition to pattern analysis [89], the ABCD rule [90] was proposed as a guideline to recognise potential melanomas in the early stages of development, using clinical and/or dermoscopic images. The ABCD abbreviation stands for the asymmetry in both in shape and color distribution, border irregularity, color variegation and large (larger than 6 mm) diameters.

Addendums and modifications to this rule have been proposed, including the newer CASH classification - color, Architecture, Symmetry, and Homogeneity [91, 92], and other rules or checklists [93], such as the Menzies rule [94] and 7-point list [95]. Evolution (E), in the sense of temporal monitoring of the skin lesion, is also a significant component in skin cancer risk assessment (Table 6).

| Rule | Feature |
|------|---------|
| *ABCD* | |
| | Asymmetry in Shape and Color |
| | Border Irregularity |
| | Color Variegation |
| | Large Diameters |
| *CASH* | |
| | Color |
| | Architecture |
| | Symmetry |
| | Homogeneity |

Table 6: Image Post-Processing – Classification by rules (examples).

Feature extraction or selection, in combination with computer-assisted classifier methods, are subsequently applied to the data in order to provide a diagnosis for malignancy. Such classification methods may be combined with fuzzy-based logic, and are generally based on machine-learning algorithms, which can be supervised (e.g., k-NN, ANN, support vector machine (SVM) and ensemble learning) or unsupervised (e.g., K-means clustering and Principle Component Analysis (PCA)). These methods may be tested on real data and compared to human diagnoses using statistical measures such as accuracy, sensitivity (recall rate) and specificity (Table 7).

| Method | Classifier |
|---|---|
| Supervised Learning | |
| | k-NN |
| | ANN |
| | SVM |
| | Ensemble Learning |
| Unsupervised Learning | |
| | K-means Clustering |
| | PCA |

Table 7: Image Post-Processing - Classifiers (examples).

Shimizu et al. [96] recently developed a novel computer-assisted method for distinguishing (melanocytic and non-melanocytic) skin lesions based on 829 candidate features related to color, sub-region and texture, and two classification models (layered and flat). The layered model was shown to provide melanoma detection rates above 90%, using an optimized selection of 25 features. An ensemble-based classification, using shape, color and texture features, was employed by Shaefer, Krawczyk & Celebi [97] and Schaefer et al. [98]. After feature selection (and retaining about 74 features), the method was shown to offer a sensitivity and specificity of over 93%. After using specialized texture analysis methods, which extracted 45 base features, a self-advising SVM algorithm, by Masood, Al-Jumaily & Anam [99], yielded an improved classification compared to standard SVM algorithms. The algorithm provided a diagnostic accuracy, sensitivity and specificity of 90%, 91% and 89%, respectively. Vasconcelos, Rosado & Ferreira [100] provided a malignancy diagnostic methodology based on the asymmetry of the skin lesion with respect to each axis of inertia. 310 asymmetry features were determined, which was then followed by feature extraction, and the application of machine-learning classification algorithms to yield an accuracy of 87% for dermoscopic images and 73,1% for hand-held device images. Celebi & Zornberg [101] applied a machine-learning approach to the automated two-class quantification (benign and malignant) of clinically significant colors in dermoscopy images, after using a K-means clustering algorithm to

reduce the number of color features. The proposed method was demonstrated to yield a sensitivity of 62% and a specificity of 76%. Takuri, Al-Kumauly & Mahmoud [102] employed a wavelet and curvelet decomposition of the grey-scale images and color features from the color images as input to a SVM algorithm. Wavelet and curvelet features provided 87.7.1% and 83.6%, 86.4% and 76.9%, and 88.1% and 85.4% accuracy, sensitivity and specificity, respectively. The RGB and L*a*b color space and respective Hue, Saturation and Intensity (HSI) and Hue, Chroma and Intensity (HCI) systems where used by Dhinagar & Celenk [103] to test their effectiveness in the diagnosis of skin cancer. The L*a*b color space was shown to yield a better classification, with an accuracy of 80%, sensitivity of 100% and specificity of 60%. In the work of Barata et al. [104], global and local classification systems were compared, using color and texture features. It was demonstrated that both classification strategies achieve satisfactory results (sensitivity = 96% and 100%, and specificity = 80% and 75%, respectively). However, color features alone were shown to outperform texture features alone, which is in contrast to previous results obtained by Rameshkumar, Santhi & Monisha [105]. A scaled-conjugate gradient-based neural network, and other neural network training algorithms, were used for the classification of skin lesions in Masood, Al-Jumaily & Aung [106] and Masood, Al-Jumaily & Adnan [107]. The best diagnostic rates that were obtained were approximately 92%.

## 6. Hand-held Device Applications

Recent years has seen a proliferation of hand-held devices and their usage, and the development of a plethora of health monitoring applications, among which are applications for skin lesion analysis. Such applications can be employed directly on the acquired high-resolution images of the device camera, or may be used in conjunction with an adaptable dermatoscopic device (e.g., for smartphones, the Handyscope[®] from FotoFinder Systems GmbH, Germany and the Dermlite

DL1® from 3Gen, Inc., USA) to improve the quality of the images. Several of these applications claim to provide accuracies and (local) processing speeds similar to algorithms implemented on common computers, while other applications upload the images and process the images on a remote server [13-18, 108, 109]. Teledermoscopy [110], the remote diagnosis of skin lesions, has also been implemented in several of these mobile applications. Below we provide some examples of these applications.

UMSkinCheck© (University of Michigan, USA) is a free application that does not perform any image processing. The idea is to provide prevention videos and literature, and notifications, while serving as a basis for storing and monitoring the skin lesions. Spotcheck® (SpotCheck Applications, Inc., USA) and Mole Detect Pro© (Lasarow Healthcare Tecnologies Limited, UK) are teledermoscopy applications that upload the skin lesion image and send it to a board-certified physician who then makes a diagnosis. SkinVision© (SkinVision B.V., The Netherlands) is the first application to employ a fractal geometry algorithm implemented on the hand-held device to provide malignancy likelihood within real-time. The application was shown to demonstrate an 81% accuracy in detecting melanoma, with 73% sensitivity and 83% specificity, compared to clinical diagnoses made by dermatologists, which presented 88% sensitivity and 97% specificity [18]. Doctor Mole© (RevoSoft, Inc., UK) and Mole Detect Pro© (Lasarow Healthcare Tecnologies Limited, UK) are applications that use the ABCDE – asymmetry, border, color, diameter, evolution – method to perform a real-time, local skin lesion analysis. DERMA/Care© [16] is a mobile application that extracts color information, and textural (e.g., entropy, contrast, variance, angular second moment) and geometric (e.g., area, perimeter, diameter) features. A SVM is then used locally to classify the skin lesion based on 32 features. SkinScan© [14] is a library that employs texture analysis and SVM to locally classify skin lesions. Testing of the procedure provided 80.76% sensitivity and 85.57% specificity, with processing speeds of about 15 seconds, comparable to many

desktop computers. Ramlakhan & Shang [15] developed a mobile system which extracts color and shape features (e.g., hull/contour ratio, circularity index), and employs a k-NN classifier for diagnosis. The results show a 66.7% accuracy, 60.7% sensitivity and 80.5% specificity for malignancy, for an average processing time of 2-5 seconds. Doukas et al. [17] present a mobile application that performs part of the image processing locally (segmentation, feature extraction, classification), but may also use a cloud service to perform the classification. After testing several classification schemes, it was concluded that SVM performed best, with a 77.06% accuracy level for benign lesions, and several classifiers (e.g., SVM) performed to an accuracy level of 85-90% for melanoma diagnosis. SKINcure[©] [109] relies on a remote server (located at the University of Bridgeport, D-Best Lab, USA) to perform image analysis. The application algorithm extracts five different features sets – 2D Fast Fourier Transform, 2D Discrete Cosine Transform, Complexity Feature Set, color Feature Set, Pigment Network Feature Set –, plus an additional four features – Lesion Shape Feature, Lesion Orientation Feature, Lesion Margin Feature and Lesion Intensity Pattern Feature. The features are then fed into a two-level classifier system for diagnosis (Table 8).

| Hand-Held Device Application/Reference | Method/Algorithm/Classifier | Processing Locale |
|---|---|---|
| UMSkinCheck[©] | Monitoring | - |
| SpotCheck[®] | Teledermoscopy | Remote |
| Mole Detect Pro[©] | Teledermoscopy | Remote |
| Mole Detect Pro[©] | ABCDE | Local |
| Doctor Mole[©] | ABCDE | Local |
| SkinVision[©] | Fractal Geometry | Local |
| DERMA/care[©] | SVM | Local |
| SkinScan[©] | SVM | Local |
| [15] | k-NN | Local |
| [17] | SVM, others | Local/Remote |
| SKINcure[©] | - | Remote |

Table 8: Hand-Held Device Applications (examples).

There have also been some recent comparative studies of several of these applications. One

such study compared the performance of four smartphone applications [108]. The sensitivity of the tested applications ranged from 6.8% to 98.1%, and specificity from 30.4% to 93.7%. It was shown that the highest sensitivity for melanoma diagnosis was obtained with an application that sends the image directly to a board-certified dermatologist for analysis (i.e., teledermoscopy). In addition, it was concluded that the performance of the applications in assessing melanoma risk was highly variable: in three of the four applications melanomas were incorrectly classified in over 30% of the cases.

## 7. Summary

We have presented a comprehensive review of the pre-processing, processing and post-processing procedures utilized in the assessment of pigmented skin lesions, with a particular emphasis on the quantification and classification of the lesions. In addition, we have reviewed and compared the major actors in mobile applications for melanoma diagnosis.

Computer-assisted state-of-the-art quantification and classification methods for skin lesion assessment, based on color, texture and shape features, and using machine-learning classifier methods, are now capable of reaching accuracy, sensitivity and specificity levels near or above 90%, comparable to the diagnostic performances provided by doctors trained in dermoscopic techniques. On the other hand, the self-diagnosis of skin lesions has been gaining popularity due to the proliferation of hand-held devices. The ever-increasing processing potential of these devices, combined with the development of high-resolution imaging cameras, has led to the development of simple affordable mobile applications that provide, in some cases, real-time skin lesion risk assessment. Indeed, several of these applications claim accuracies and local processing speeds (a few seconds) comparable to those provided by running image processing algorithms on common computers. However, it is found that in over 30% of the cases, melanomas may be incorrectly

classified using these locally-processed mobile applications, a percentage far too high to provide a safe and feasible alternative to a specialist examination and diagnosis. In fact, of all the mobile applications that were tested in literature, it was found that the ones that employ teledermoscopy (e.g., remote skin lesion diagnosis using a board-certified physician) still provide the best statistical measures (over 90%) for malignancy assessment.

Thus, although some mobile applications do show promise, the crucial, complex and computationally heavy quantification and classification step of skin lesion analysis continues to pose a significant challenge to the creation of a real-time application that will allow an accurate assessment of melanoma cases.

**References**

[1] Cakir, B. O., Adamson, P. & Cingi, C., "Epidemiology and economica burden of nonmelonoma skin cancer", Facial Plastic Surgery Clinics of North America, 20, 419-422, 2012

[2] Dubas, L. E. & Ingraffea, A., "Nonmelanoma skin cancer", Facial Plastic Surgery Clinics of North America, 21, 43-53, 2013

[3] World Cancer Report, World Health Organization, Chapter 5.14, ISBN 9283204298, 2014

[4] Lozano, R. et al., "Global and regional mortality from 235 causes of death for 20 age groups in

1990 and 2010: a systematic analysis for the Global Burden of Disease Study 2010", The Lancet, 380, 2095-2128, 2011

[5] Wang, S. W. et al., "Current technologies for the in vivo diagnosis of cutaneous melanomas", Clinics in Dermatology, 22(3), 217-222, 2004

[6] Ruocco, E. et al. "Noninvasive imaging of skin tumors", Dermatologic Surgery, 30, 301-310, 2004

[7] Smith, L. & MacNeil, S., "State of the art in non-invasive imaging of cutaneous melanoma", Skin Research and Technology, 17(3), 257-269, 2011

[8] Lorentzen, H., Weismann, K., Petersen, C. S., Larsen, F. G., Secher, L. & Skodt, V., "Clinical and dermoscopic diagnosis of malignant melanoma. Assessed by expert and non-expert groups", Acta Dermato-Venereologica, 79(4), 301-304, 1999

[9] Ascierto, P. A. et al., "Sensitivity and specificity of epiluminiscence miscroscopy: evaluation on a sample of 2731 excised cutaneous pigmented lesions", British Journal of Dermatology, 142, 893-898, 2000

[10] Vestergaard, M. E., Macaskill, P., Holt, P. E. & Menzies, S. W., "Dermoscopy compared with naked eye examination for the diagnosis of primary melanoma: a meta-analysis of studies performed in a clinical setting", British Journal of Dermatology, 159, 669-676, 2008

[11] Zortea, M., Schopf, T. R., Thon, K., Geilhufe, M., Hindberg, K., Kirchesch, H., Mollerson, K., Schulz, J., Skrovseth, S. O. & Godtliebsen, F., "Performance of a dermoscopy-based computer vision system for the diagnosis of pigmented skin lesions compared with visual evaluation by experienced dermatologists", Artificial Intelligence in Medicine, 60, 13-26, 2014

[12] Skvara, H., Burnett, P., Jones, J., Duschek, N., Plassmann, P. & Thirion, J. P., "Quantification of skin lesions with a 3D stereovision camera system: validation and clinical applications", Skin Research and Technology, 19, 182-190, 2013

[13] Zouridakis, G. Wadhawan, T., Situ, N., Hu, R., Yuan, X., Lancaster, K. & Queen, C. M., "Melanoma and other skin lesion detection using smart Hand-Held devices", Methods in Molecular Biology, 1256, 459-496, 2015

[14] Wadhawan, T., Situ, N., Lancaster, K., Yuan, X. & Zouridakis, G., "SkinScan$^©$: A portable library for melanoma detection on Hand-Held devices," IEEE International Symposium on Biomedical Imaging: From Nano to Macro, 133-136, 2011

[15] Ramlakhan, K. & Shang, Y., "A Mobile Automated Skin Lesion Classification System," 23rd IEEE International Conference on Tools with Artificial Intelligence, 138-141, 2011

[16] Karargyris, A., Karargyris, O. & Pantelopoulos, A., "DERMA/care: An advanced image-processing mobile application for monitoring skin cancer," IEEE 24th International Conference on Tools with Artificial Intelligence, 1-7, 2012

[17] Doukas, C., Stagkopoulos, P., Kiranoudis, C. & Maglogiannis, I., "Automated skin lesion assessment using mobile technologies and cloud platforms," IEEE Annual Conference, Engineering in Medicine and Biology Society, 2444-2447, 2013

[18] Maier, T., Kulichova, D., Schotten, K., Astrid, R., Ruzicka, T., Berking, C. & Udrea, A., "Accuracy of a smartphone application using fractal image analysis of pigmented moles compared to clinical diagnosis and histological result", Journal of the European Academy of Dermatology and Venereology, 29(4), 663-667, 2015

[19] Bankman, I. N. (editor), Handbook of Medical Imaging: Processing and Analysis, Academic Press Series, 910 pp., 2000

[20] Gonzalez, R. C. & Woods, R. E., Digital Image Processing, 2nd ed., New Jersey: Prentice Hall, 190 pp., 2002

[21] Perona, P. & Malik, J., "Scale-space and edge detection using anisotropic diffusion", IEEE Transactions on Pattern Analysis and Machine Intelligence, 12(7), 629-639, 1990

[22] Sonka, M, Hlavac, V. & Boyle, R., Image Processing, Analysis, and Machine Vision, 2nd. ed., PWS, 800 pp., 1998

[23] Tomasi, C. & Manduchi, R., "Bilateral filtering for gray and color images," IEEE International Conference on Computer Vision, 839-846, 1998

[24] Butt, I. & Rajpoot, N., "Multilateral filtering: A novel framework for generic similarity-based image denoising," IEEE International Conference on Image Processing, 2981-2984, 2009

[25] Zhang, M., "Bilateral Filter in Image Processing," Master's Thesis, Louisiana State University, Baton Rouge, LA, 2009

[26] Al-Abayechi, A. A. A., Logeswaran, R., Xiaoning Guo, & Wooi-Haw Tan, "Lesion border detection in dermoscopy images using bilateral filter", IEEE International Conference on Signal and Image Processing Applications, 365-368, 2013

[27] Silveira, M. et al. "Comparison of segmentation methods for melanoma diagnosis in dermoscopy images", IEEE Journal of Selected Topics in Signal Processing, 3(1), 35-45, 2009

[28] Uemura, T., Koutaki, G. & Uchimura, K., "Image segmentation based on edge detection using boundary code", International Journal of Innovative Computing, Information and Control, 7(10), 11 pp., 2011

[29] Canny, J., "A computational approach to edge detection", IEEE Transactions on Pattern Analysis and Machine Intelligence, 8(6), 679-698, 1986

[30] Yasmin, J. H. J., Sathik, M. M., Beevi, S. Z., "Effective border detection of noisy real skin lesions for skin lesion diagnosis by robust segmentation algorithm", International Journal of Advanced Research in Computer Science, 1(3), 110-115, 2010

[31] Yasmin, J. H. J. & Sadiq, M. M., "An improved iterative segmentation algorithm using Canny edge detector with iterative median filter for skin lesion border detection", International Journal of Computer Applications, 50(6), 37-42, 2012

[32] Al-Amri, S. S., Kalyankar, N. V. & Khamitkar, S. D., "Image segmentation by using threshold techniques", Journal of Computing, 2(5), 1-4, 2010

[33] Abbas, A. A. Guo, X., Tan, W. H. & Jalab, H. A., "Combined spline and B-spline for an improved automatic skin lesion segmentation in dermoscopic images using optimal color channel systems-level quality improvement", Journal of Medical Systems, 28, 1-8, 2014

[34] Otsu, N., "A threshold selection method from gray-level histograms", IEEE Transactions on Systems, Man and Cybernetics, 9(1), 62-66, 1979

[35] Garnavi, R., Aldeen, M., Celebi, M. E., Varigos, G. & Finch, S., "Border detection in dermoscopy images using hybrid thresholding on optimized color channels", Computerized Medical Imaging and Graphics, 35(2), 105-115, 2011

[36] Gould, S., Gao, T. & Koller, D., "Region-based segmentation and object detection", Advances in Neural Information Processing Systems, 655-663, 2009

[37] Mumford, D. & Shah, J., "Optimal approximations by piecewise smooth functions and associated variational problems", Communications on Pure and Applied Mathematics, 42(5), 577-685, 1989

[38] Chan, T. F. & Vese, L. A., "Active contours without edges" IEEE Transactions on Image Processing, 10(2), 266-277, 2001

[39] Capdehourat, G., Corez, A., Bazzano, A., Alondo, R. & Musé, P., "Toward a combined tool to assist dermatologists in melanoma detection from dermoscopic images of pigmented skin lesions", Pattern Recognition Letters, 32(16), 2187-2196, 2011

[40] Oliveira, R. B., Tavares, J. M. R. S., Marranghello, N. & Pereira, A. S., "An Approach to Edge Detection in Images of Skin Lesions by Chan-Vese Model", 8th Doctoral Symposium in Informatics Engineering, Oporto, 1, 2013

[41] Rastgarpour, M. & Shanbehzadeh, J., "The Status Quo of Artificial Intelligence Methods in

Automatic Medical Image Segmentation", International Journal of Computer Theory and Engineering, 5(1), 4 pp., 2013

[42] Haykin, S. S., "Neural networks: A comprehensive foundation", Prentice Hall, 842 pp., 1999

[43] Haupt, R. L. & Haupt, S. E. "Practical genetic algorithms", 2nd ed., New Jersey: John Wiley & Sons, 253 pp., 2004

[44] Aswin, R. B. "Hybrid genetic algorithm - Artificial neural network classifier for skin cancer detection", International Conference on Control, Instrumentation, Communication and Computational Technologies, 1304-1309, 2014

[45] Kass, M., Witkin, A. & Terzopoulos, D., "Snakes: Active contour models", International Journal of Computer Vision, 1(4), 321-331, 1988

[46] Xu, C. & Prince, J. L., "Snakes, shapes, and gradient vector flow", IEEE Transactions on Image Processing, 7(3), 359-369, 1998

[47] Zhou, H., Schaefer, G., Celebi, M., Iyatomi, H., Norton, K. A., Liu, T., & Lin, F., "Skin lesion segmentation using an improved snake model", IEEE Annual International Conference on Engineering in Medicine and Biology Society, 1974-1977, 2010

[48] Osher, S. & Sethian, J. A., "Fronts propagating with curvature-dependent speed: Algorithms based on hamilton-jacobi formulations", Journal of Computational Physics, 79(1), 12-49, 1988

[49] Ma, Z. & Tavares, J. M. R. S., "Segmentation of Skin Lesions Using Level Set Method", Computational Modeling of Objects Presented in Images: Fundamentals, Methods, and Applications, 228-233, 2014

[50] Maeda, J., Kawano, A., Sato, S. & Suzuki, Y., "Number-driven perceptual segmentation of natural color images for easy decision of optimal result", IEEE International Conference on Image Processing, 2, 265-268, 2007

[51] Maeda, J., Kawano, A., Sato, S. & Suzuki, Y., "Unsupervised perceptual segmentation of

natural color images using fuzzy-based hierarchical algorithm" Image analysis, Lecture Notes in Computer Science, Springer, Volume 4522, 462-471, 2007

[52] Maeda, J., Kawano, A., Yamauchi, S., Suzuki, Y., Marçal, A. R. S. & Mendonça, T., "Perceptual image segmentation using fuzzy-based hierarchical algorithm and its application to dermoscopy images" IEEE Conference on Soft Computing in Industrial Applications, 66-71, 2008

[53] Rahman, M. M., Bhattacharya, P. & Desai, B. C., "A multiple expert-based melanoma recognition system for dermoscopic images of pigmented skin lesions", 8th IEEE International Conference on BioInformatics and BioEngineering, 1-6, 2008

[54] Castiello, C., Catellano, G. & Fanelli, A. M., "Neuro-fuzzy analysis of dermatological images", IEEE International Joint Conference on Neural Networks, 4, 3247-3252, 2004

[55] Mendel, H. M. & John, R. I. B., "Type-2 fuzzy sets made simple", IEEE Transactions on Fuzzy Systems, 10(2), 117-127, 2002

[56] Cover, T. & Hart, P., "Nearest neighbor pattern classification", IEEE Transactions on Information Theory, 13(1), 21-27, 1967

[57] Ballerini, L., Fisher, R. B., Aldridge, B. & Rees, J., "A color and texture based hierarchical k-NN approach to the classification of non-melanoma skin lesions", Lecture Notes in Computational Vision and Biomechanics, Volume 6, 63-86, 2013

[58] John, J. M., Samual, S. S. & John, N. M., "Segmentation of skin lesions from digital images using texture distinctiveness with neural network", International Journal of Advanced Research in Computer and Communication Engineering, 3(8), 7777-7780, 2014

[59] Lloyd, S. P., "Least squares quantization is PCM", IEEE Transactions on Information Theory, 28(2), 129-137, 1982

[60] Ma, Z. & Tavares, J. M. R. S., "A novel approach to segment skin lesions in dermoscopic images based on a deformable model", IEEE Journal on Biomedical Health Information, DOI:

10.1109/JBHI.2015.2390032, 2015

[61] Sirakov, N. M., Ou, Y. -L. & Mete, M., "Skin lesion feature vectors classification in models of a Riemannian manifold", Annals of Mathematics and Artificial Intelligence, 2-15, 2014

[62] Hunter, R. S., "Photoelectric Color-Difference Meter", Journal of the Optical Society of America, 38(7), 661, 1948

[63] Gevers, T., van der Weijer, J. & Stokman, H., "Color feature detection", Color Image Processing: Emerging Applications, R. Lukac & K. N. Plataniotis eds., Chapter 1, CRC Press, 1-27, 2006

[64] White, R., Rigel, D. S. & Friedman, R., "Computer Applications in the Diagnosis and Prognosis of Malignant Melanoma," Dermatologic Clinics, 9, 695-702, 1992

[65] Hu, M. - K., "Visual pattern recognition by moment invariants", IRE Transactions on Information Theory, 179-187, 1967

[66] Mertzios, B. G. & Tsirikolias, K., "Statistical shape discrimination and clustering using an efficient set of moments", Pattern Recognition Letters, 14, 517-522, 1993

[67] Gutkowicz-Krushin, D., Elbaum, M., Szwaykowski, P. & Kopf, A. W., "Can early malignant melanoma be differentiated from atypical melanocytic nevus by invivo techniques?", Skin Research and Technology, 3, 15-22, 1997

[68] Mallat, S., "A theory of multi-resolution signal decomposition: the wavelet representation", IEEE Transactions on Pattern Analysis and Machine Intelligence, 11, 674-693, 1989

[69] Gopinath, R. A. & Burrus, C. S., "Wavelet transforms and filter banks", Wavelets – A Tutorial in Theory and Applications, C. K. Chui ed., Academic Press, San Diego, 603-654, 1992

[70] Easton Jr., R. L., "Fourier Methods in Imaging", Wiley, 954 pp., 2010

[71] Kim, S. D., Lee, J. H. & Kim, J. K., "A new chain-coding algorithm for binary images using run-length codes", Computer Vision Graphics Image Processing, 41, 114-128, 1988

[72] Davidson, J. "Thinning and skeletonizing: A tutorial and overview", Digital Image Processing: Fundamental and Applications, E. Dougherty ed., Marcel Dekker, New York, 1991

[73] Lam, L., Lee, S. & Suen, C., "Thinning methodologies − A comprehensive survey", IEEE Transactions on Patter Analysis and Machine Intelligence, 14, 868-885, 1992

[74] Zhang, T. Y. & Suen, C. Y., "A fast parallel algorithm for thinning digital patterns", Communications of the Association for Computing Machinery, 27(3), 236-239, 1984

[75] Tuceryan, M., "Moment based texture segmentation", Pattern Recognition Letters, 15, 659-668, 1994

[76] Haralick, R. M., Shanmugam, K. & Dinstein, I., "Textural features for image classification", IEEE Transactions on Systems, Man and Cybernetics, 3, 610-621, 1973

[77] Handels, H., Ross, T., Kreusch, J., Wolff, H. H. & Poppl, S. J., "Computer-supported diagnosis of melanoma in profilometry", Methods of Information in Medicine, 38, 43-49, 1999

[78] Shanmugavadivu, P. & Sivakumar, V., "Fractal Dimension Based Texture Analysis of Digital Images", Procedia Engineering, International Conference on Modelling Optimization and Computing, 38, 2981-2986, 2012

[79] Barnsley, M., "Fractals Everywhere", Toronto, Canada, Academic Press, 1988

[80] Lundhal, T., Ohley, W. J., Kay, S. M. & Siffert, R., "Fractional Brownian motion: a maximum likelihood estimator and its applications to image texture", IEEE Transactions on Medical Imaging, 5, 152-161, 1989

[81] Penn, A. I. & Loew, M. H., "Estimating fractal dimension with fractal interpolation function models", IEEE Transactions on Medical Imaging, 16, 930-937, 1997

[82] Nailon, W. H. (2010), "Texture Analysis Methods for Medical Image Characterisation", Biomedical Imaging", Youxin Mao (Ed.), 27 pp., 2010

[83] Clawson, K. M. et al., "Determination of optimal axes for skin lesion asymmetry

quantification", IEEE International Conference on Image Processing, 2, 453-456, 2007

[84] Tosca, A. et al., "Development of a three-dimensional surface imaging system for melanocytic skin lesion evaluation", Journal of Biomedical Optics, 18(1), 13 pp., 2013

[85] Delibasis, K., Undrill, P. E. & Cameron, G. G., "Designing Fourier descriptor based geometric models for object interpretation in medical images using genetic algorithms", Computer Vision and Image Understanding, 66, 286-300, 1997

[86] Naf, M., Szekely, G., Kikinis, R., Shenton, M. E. & Kubler, O., "3D Vornoi skeletons and their usage for the characterization and recognition of 3D organ shape", Computer Vision and Image Understanding, 66, 147-161, 1997

[87] Palagyi, K. & Kuba, A. "A hybrid thinning algorithm for 3D medical images", Journal of Computing and Information Technology, 6, 149-164, 1998

[88] Zhou, Y. & Toga, A. W., "Efficient skeletonization of volumetric objects", IEEE Transactions on Visualization and Computer Graphics, 5, 196-209, 1999

[89] Pehamberger, H., Steiner, A. & Wolff, K., "In vivo epiluminescence microscopy of pigmented skin lesions. I. Pattern analysis of pigmented skin lesions", Journal of the American Academy of Dermotology, 17(4), 571-583, 1987

[90] Friedman, R. J., Rigel, D. S. & Kopf, A. W., "Early detection of malignant melanoma: the role of physician examination and self-examination of the skin", A Cancer Journal for Clinicians, 35(3), 130-51, 1985

[91] Henning, J. S., "The CASH (color, architecture, symmetry, and homogeneity) algorithm for dermoscopy", Journal of the American Academy of Dermatology, 56, 45-52, 2007

[92] Henning, J. S., Stein, J. A., Yeung, J. & Dusza, J. W., "CASH algorithm for dermoscopy revisited", Archives of Dermatology, 144, 554-555, 2008

[93] Johr, R. H., "Dermoscopy: alternative melanocytic algorithms - the ABCD rule of

dermatoscopy, menzies scoring method, and 7-point check-list", Clinics in Dermatology 20, 240-247, 2002

[94] Menzies, S. W., Ingvar, C., Crotty, K. A. & McCarthy, W. H., "Frequency and morphologic characteristics of invasive melanomas lacking specific surface microscopic features", Archives of Dermatology, 132(10), 1178–1182, 1996

[95] Argenziano, G., Fabbrocini, G., Carli, P. & De Giorgi, V., "Epiluminescence microscopy for the diagnosis of doubtful melanocytic skin lesions" Archives of Dermatology, 134, 1563-70, 1998

[96] Shimizu, K., Iyatomi, H., Celebi, M. E., Norton, K. A. & Tanaka, M., "Four-class classification of skin lesions with task decomposition strategy", IEEE Transactions on Biomedical Engineering, 62, 274-283, 2015

[97] Schaefer, G. Krawczyk, B., Celebi, M. E. & Iyatomi, H. "An ensemble classification approach for melanoma diagnosis", Memetic Computing, 6(4), 223-240, 2014

[98] Schaefer, G., Krawczyk, B., Celebi, M. E., Iyatomi, H. & Hassanien, A. E., "Melanoma classification based on ensemble classification of dermoscopy image features", Communications in Computer and Information Science, 488, 291-298, 2014

[99] Masood, A., Al-Jumaily, A. & Anam, K., "Texture analysis based automated decision support system for classification of skin cancer using SA-SVM", Lecture notes in computer science, Springer, Volume 8835, 101-109, 2014

[100] Vasconcelos, M. J. M., Rosado, L. & Ferreira, M., "Principal axes-based asymmetry assessment methodology for skin lesion image analysis", Lecture Notes in Computer Science, Springer, Volume 8888, 21-31, 2014

[101] Celebi, M. E. & Zomberg, A., "Automated quantification of clinically significant colors in dermoscopy images and its application to skin lesion classification", IEEE Systems Journal, 8, 980-984, 2014

[102] Takuri, M., Al-Jumaily, A. & Mahmoud, M. K. A., "Automatic recognition of melanoma using Support Vector Machines: A study based on Wavelet, Curvelet and color features", Proceedings of the International Conference on Industrial Automation, Information and Communications Technology, 70-75, 2014

[103] Dhinagar, N. J. & Celenk, M., "Performance assessment of the use of the RGB and LAB color spaces for non-invasive skin cancer classification", 29th International Conference on Computers and Their Applications, 243-248, 2014

[104] Barata, C., Ruela, M., Francisco, M., Mendonça, T. & Marques, J. S., "Two systems for the detection of melanomas in dermoscopy images using texture and color features", IEEE Systems Journal, 8(3), 965-979, 2014

[105] Rameshkumar, P., Santhi, B. & Monisha, M., "Significance of color & texture features in computerized melanoma diagnosis using soft computing techniques", International Journal of Applied Engineering Research, 9(12), 1875-1884, 2014

[106] Masood, A., Al-Jumaily, A. & Aung, Y. M., "Scaled conjugate gradient based decision support system for automated diagnosis of skin cancer", Proceedings of the IASTED International Conference on Biomedical Engineering, 196-203, 2014

[107] Masood, A., Al-Jumaily, A. & Adnan, T., "Development of automated diagnostic system for skin cancer: Performance analysis of neural network learning algorithms for classification", Lecture Notes in Computer Science, Volume 8681, 837-844, 2014

[108] Wolf, J. A., Moreau, J. F., Akilov, O., Patton, T., English III, J. C., Ho, J. & Ferris, L. K., "Diagnostic Inaccuracy of Smartphone Applications for Melanoma Detection", Journal of the American Medical Association Dermatology, 149(4), 422-426, 2013

[109] Abuzaghleh, O., Faezipour, M. & Barkana, B. D., "Skincure: An Innovative Smart Phone-Based Application To Assist In Melanoma Early Detection And Prevention", Signal & Image

Processing: An International Journal, DOI: 10.5121/sipij.2014.5601, 5(6), 15 pp., 2014

[110] Massone, C., Brunasso, A. M., Campbell, T. M. & Soyer, H. P., "Mobile teledermoscopy- melanoma diagnosis by one click?," Seminars in Cutaneous Medicine and Surgery, 203-205, 2009